

Modelling Al-4wt.%Cu as-cast structure using equiaxed morphological parameters deduced from in-situ synchrotron X-ray radiography

This content has been downloaded from IOPscience. Please scroll down to see the full text.

2016 IOP Conf. Ser.: Mater. Sci. Eng. 117 012010

(<http://iopscience.iop.org/1757-899X/117/1/012010>)

View [the table of contents for this issue](#), or go to the [journal homepage](#) for more

Download details:

IP Address: 193.170.16.107

This content was downloaded on 01/04/2016 at 14:03

Please note that [terms and conditions apply](#).

Modelling Al-4wt.%Cu as-cast structure using equiaxed morphological parameters deduced from in-situ synchrotron X-ray radiography

M Ahmadein^{1,2,a}, M Wu^{1,3,b}, G Reinhart^{4,5}, H Nguyen-Thi^{4,5} and A Ludwig¹

¹ Chair for Modeling and Simulation of Metallurgical Processes, University of Leoben, Austria

² Department of Production Engineering and Mech. Design, Tanta University, Egypt

³ Christian-Doppler Laboratory for Advanced Process Simulation of Solidification & Melting, University of Leoben, Austria

⁴ Aix-Marseille University & ⁵ CNRS, IM2NP UMR 7334, Campus Saint-Jérôme, Case 142, 13397 Marseille Cedex 20, France

Email: ^a mahmoud.ahmadein@unileoben.ac.at, ^b menghuai.wu@unileoben.ac.at

Abstract. The as-cast structure of laboratory scale Al-4wt.%Cu was numerically calculated using assumed morphological parameters. Two parameters are identified: The shape factor which correlates the growth velocity of dendrite envelope to that of the tip; and the sphericity of the equiaxed envelope or the circularity of the columnar trunk envelope which is required to calculate the averaged species diffusion flux across the envelope. In the present work, the real-time radiographs of equiaxed solidification experiment carried out on Al-4wt.%Cu at the European Synchrotron Radiation Facility are used to track the development of crystal envelope with time. The growth rate of the equivalent circular envelope was correlated to dendrite tip growth velocity to deduce the shape factor. The sphericity of dendrite envelope is estimated over the time. The average of the deduced morphological parameters is applied to the model to predict the as-cast structure. The results were compared to those obtained by using morphological parameters from literature. The predicted phase quantities, columnar-to-equiaxed transition, and macrosegregation exhibited significant dependence on those parameters. The predicted macrosegregation using the experimentally deduced parameters fits better to the measurements.

1. Introduction

Modelling the formation of the solidification structure is an essential tool to control the mechanical properties of a specific alloy. Numerous models have been proposed over decades. However, few of them can be applied on process scale. Beckermann and co-workers [1,2] used a multiphase, volume-averaged approach to incorporate the microscopic crystal growth kinetics into the macroscopic model for the transport phenomena occurring at the process scale. Rappaz and Thévoz [3,4] proposed a micro-macro model to incorporate the dendritic crystal morphology into the global transport system. The columnar-to-equiaxed transition (CET) was also treated in several works [5-7], but the growth of the columnar dendrites were over-simplified. More sophisticated 3-phase model dealing with mixed columnar-equiaxed solidification was proposed by some of the current authors [8-10]. It was demonstrated that it can account for melt convection and grain sedimentation, macrosegregation, and macrostructure. They extended their model to a 5-phase one that incorporates the dendritic growth of the columnar and equiaxed crystals [11,12]. The 5-phase model was verified to be able to



quantitatively predict the as-cast structure of Al-alloy ingots [13,14] and the solidification and melt flow of the ammonium chloride transparent solution [15].

On continued trials to improve the quantitative results of the 5-phase model, the present work is devoted to evaluate the influence of morphological parameters on simulation results. Real-time radiographs of the equiaxed solidification experiment carried out on Al-4wt.%Cu at the European Synchrotron Radiation Facility was used to track the development of crystal envelope with time. The average shape factor and the sphericity of the equiaxed crystals are determined. The predicted results using morphological parameters from literature and those deduced from the current experiment are compared and discussed.

2. Modelling aspects

The 5-phase mixed columnar-equiaxed solidification model with dendritic morphology comprises three hydrodynamic phases: the liquid melt, the equiaxed crystals, and the columnar grains, denoted as e -, c - and l -phases and have corresponding volume fractions; f_l , f_e , and f_c . Globular and dendritic growth of equiaxed crystals and cellular and dendritic growth of columnar grains are considered. In case of dendritic growth, two additional phase regions exist within each of the equiaxed and the columnar crystal envelopes as shown in figure 1: the solid dendrites with corresponding solid fractions α_s^e and α_s^c , and interdendritic melt with corresponding volume fractions α_d^e and α_d^c inside crystal envelopes. It is assumed that the interdendritic melt is transported with the solid dendrites and is generally more solute-enriched than the extradendritic melt surrounding the crystals. In this sense, a fictitious crystal boundary envelope is constructed to separate the interdendritic melt from the extradendritic melt. Consequently, the system encompasses five ‘thermodynamic’ phases: (1) the solid dendrite and (2) the interdendritic melt within the equiaxed grain, (3) the solid dendrite and (4) interdendritic melt within the columnar crystal envelope, and (5) the extradendritic melt. The corresponding averaged volume fractions are: f_s^e , f_d^e , f_s^c , f_d^c , f_l referring to total volume and they characterize by corresponding solute concentration: c_s^e , c_d^e , c_s^c , c_d^c , c_l .

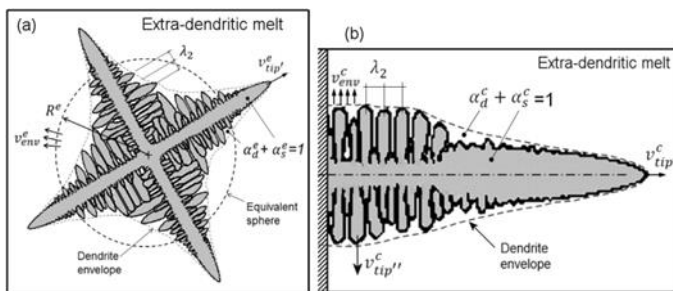


Figure 1. Schematic of the dendrite envelope separating the inter- and extra-dendritic melt for the (a) equiaxed crystal and (b) columnar dendrite.

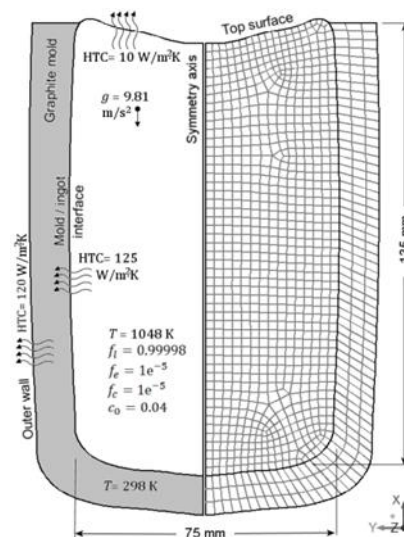


Figure 2. 2D-axisymmetric grid boundary and initial conditions of the ingot casting.

The growth of the grain envelope and the solidification of the interdendritic melt are treated differently. The growth of the envelopes is determined by dendrite growth kinetics. The semi-empirical Kurz-Giovanola-Trivedi (KGT) model [16] is used for the growth of columnar primary dendrite tips with velocity, v_{tip}^c . Lipton-Glicksman-Kurz (LGK) model [17] is applied for the

growth of columnar secondary dendrite tips (radial growth of the columnar trunk) and equiaxed primary dendrite tips. The profiles of the equiaxed grain and columnar trunk envelopes are respectively simplified as volume-equivalent sphere with radius R^e and volume-equivalent cylinder with radius R^c . For equiaxed crystals a shape factor, φ_{env}^e , correlates the growth velocity of the equivalent sphere, v_{env}^e , to the primary dendrite tip velocity, v_{tip}^e , as given in equation (1). Similarly, φ_{env}^c for the columnar trunk correlates v_{env}^c to v_{tip}^c , as given in equation (2). To calculate the species diffusive flux across the grain envelope, the real surface area of equiaxed and columnar envelopes, S_{env}^e and S_{env}^c , is respectively correlated to the surface area of equivalent sphere, S_{sph}^e , and the equivalent cylinder, S_{cyl}^c , by a sphericity form factor, φ_{sph}^e , for the equiaxed grain and a circularity shape factor, φ_{circ}^c , for the columnar trunk as given in equations (3) and (4), respectively.

$$v_{env}^e = \varphi_{env}^e \cdot v_{tip}^e \quad (1)$$

$$v_{env}^c = \varphi_{env}^c \cdot v_{tip}^c \quad (2)$$

$$S_{env}^e = S_{sph}^e / \varphi_{sph}^e \quad (3)$$

$$S_{env}^c = S_{cyl}^c / \varphi_{circ}^c \quad (4)$$

A heterogeneous nucleation law [18,19] is used to calculate the source term for the transport equation of the equiaxed number density. The advancement of the columnar tip front can be prevented either mechanically (hard blocking) when f_e ahead of the columnar primary tip front exceeds 0.49 [21] or thermodynamically (soft blocking) [6] when liquid melt at the columnar tip is enriched with solute to the extent that the constitutional undercooling vanishes. At this moment columnar-to-equiaxed (CET) transition occurs. Further details of the model are provided in [11,20].

The above model is used to predict the solidification structure of a cylindrical Al-4.0wt.%Cu ingot in a graphite mould using a 2D axisymmetric grid as shown in figure 2. The temperature of mould and melt were initially set to 298 K and 1048 K respectively. The thermophysical properties and the modelling parameters of the alloy are provided in [14]. The conservation equations of mass, enthalpy, species, and number density are solved using CFD software package, ANSYS-Fluent version 14.5.0 based on the control volume method. The time step size to achieve the solution convergence during a solidification time of ~525 s ranged between 1×10^{-5} and 1×10^{-3} s.

Five simulation cases were conducted to study the influence of the morphological parameters on the predicted as-cast structure using assumed, literature, and measured morphological parameters as listed in table 1. Real-time radiographs of equiaxed solidification experiment carried out on Al-4wt.%Cu are used to determined φ_{env}^e and φ_{sph}^e as explained in the next section.

Table 1. Morphological parameters of the dendritic envelope from different sources.

Study cases	φ_{env}^e	φ_{sph}^e	φ_{env}^c	φ_{circ}^c	Source
Case#1	0.48 ^a	0.4 ^a	0.798 ^a	0.5 ^a	^a Assumed
Case#2	0.683 ^b	0.846 ^b	0.798 ^b	0.886 ^b	^b Equiaxed: octahedral, columnar: square rod [11]
Case#3	0.478 ^c	0.837 ^c	0.564 ^c	0.56 ^c	^c Equiaxed: 6 orthogonal square pyramids,
Case#4	0.358 ^d	0.623 ^d	0.798 ^b	0.886 ^b	columnar: 4 orthogonal square wedges [11]
Case#5	0.358 ^d	0.623 ^d	0.564 ^c	0.56 ^c	^d Current experiment

3. Determination of equiaxed morphological parameters

Directional solidification experiments were carried out on beamline ID19 at the European Synchrotron Radiation Facility (ESRF, Grenoble, France). The sample was made of an Al-4wt.%Cu alloy, 35 mm in length, 6 mm in width and 150-200 μm in thickness. The sample was adjusted into a soft graphite crucible designed to somewhat accommodate the thermal expansion stresses in the region surrounding the solid-liquid interface. The details of the used Bridgman furnace have been described in [23]. The

applied temperature gradient G between the two heaters was set to 17.5 K/cm and anti-parallel to gravity. Solidification was triggered by decreasing the temperature of the hot zone at a rate of 1 K/min, while maintaining the same injected power to the bottom heater. To trigger the CET the temperature gradient is continuously decreased to 10 K/cm. Radiographs of the solidifying samples were recorded with an ESRF FReLoN (Fast Read-out Low Noise) camera. Details about the used optics, beam energy and image processing can be found in [24]. The final result is enhanced contrast and almost defect free images with the solidified Al-rich structures appearing in light grey and the Cu-rich liquid regions appearing in dark grey as shown in figure 1.

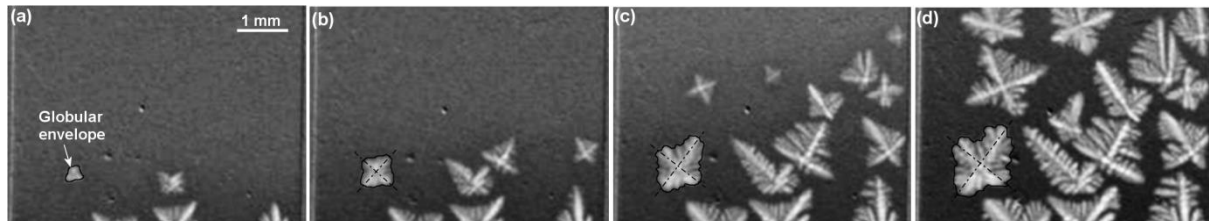


Figure 3. In situ radiographs of equiaxed solidification of Al-4wt.-% Cu at relative times (a) 0 s, (b) 45 s, (c) 126 s, and (d) 225 s, with cooling from the bottom at a rate of 0.5 K/min.

To determine φ_{env}^e and φ_{sph}^e , the growth of primary dendrite tip and the evolution of dendrite envelope are traced over the solidification time. 2D real-time radiographs of the growing equiaxed crystals from the above experiment are used for this purpose. An example of tracing the envelope development is shown in figure 1. The following procedure is applied to four crystals: (1) the most equiaxially growing crystals are selected, (2) evaluation starts from the onset of crystal growth and ends before grain impingement, (3) two main growth axes and a dendrite envelope are drawn for each crystal, (4) the radius of the equivalent-area circle, R^e , is calculated, (5) from the length development of the each of the dendritic axes, v_{tip}^e is calculated as the average of both, (6) from the development of R^e over time, v_{env}^e is calculated, (7) equation (1) is applied at each time to get φ_{env}^e , (8) φ_{sph}^e is calculated as the ratio of the perimeter of the equivalent-area circle to the perimeter of the actual dendrite envelope.

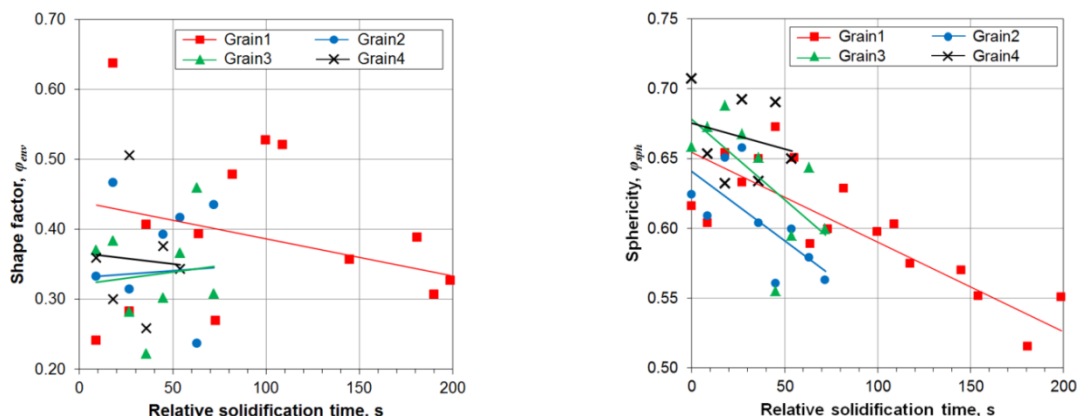


Figure 4. Discrete measurements and trend lines of (a) shape factor (b) sphericity of equiaxed envelope during solidification of Al-4wt.-%Cu alloy.

The development of φ_{env}^e and φ_{sph}^e is plotted for the 4 crystals versus solidification time as shown in 2a and b, respectively. The measured φ_{env}^e and φ_{sph}^e are fluctuating with time, in contradiction with the assumptions of the 5-phase model [11]. This can be attributed to melt flow and the unsteady solute distribution in the liquid ahead of the dendrite tips, which affects the tip undercooling and correspondingly the growth rate and envelope morphology. The resulting φ_{env}^e is more fluctuating

than φ_{sph}^e because it is calculated directly from v_{tip}^e , which is very sensitive to the tip undercooling. In general, φ_{sph}^e decreases with time. High φ_{sph}^e is an evidence for the globular growth at the beginning of solidification as shown in 2b. As solidification proceeds the morphology tends to be more dendritic. As a result, φ_{sph}^e decreases. For modelling purpose, a constant value of $\varphi_{env}^e = 0.358$ and $\varphi_{sph}^e = 0.623$ are considered by averaging the measurements of the four crystals over the time.

4. Simulation results

The as-cast structure is calculated using 5 sets of morphological parameter as per table 1. The resulting CET lines are overlaid on the as-cast structure from experiment as shown in figure 5. The as-cast structure for all cases comprises an equiaxed core, columnar top and ingot peripherals, and a CET surface. Compared to the top CET boundary, the bottom CET boundary is almost unaffected. Nevertheless, the proportion of each phase region differs depending on the morphological parameters.

Some averaged phase quantities in the ingot and inside the CET surface are listed in table 2. By comparing the results (case#2 vs. case#4) and (case#3 vs. case#5), it can be easily concluded that, as φ_{env}^e decreases, the formed fraction of equiaxed phase in ingot, f_e decreases. This can be attributed to the reduction of the growth rate of the equiaxed grain envelope v_{env}^e according to equation (1).

The sphericity of the equiaxed crystal in the 5-phase model is directly correlated to the envelope diffusion area as given in equation (3). The smaller the sphericity (i.e. more dendritic morphology) the higher the diffusion surface concentration, S_{env}^e and correspondingly, the diffusion flux through the grain envelope increases. By increasing S_{env}^e a higher species transport rate is expected from the solute-rich interdendritic liquid to the less enriched extradendritic liquid. As a result, inside the dendrite envelope the formed eutectic (residual liquid) fraction, α_d^e , decreases and the solid fraction, α_s^e , increases. This is obvious from the results listed in table 2, where φ_{sph}^e decreases from 0.846 to 0.623 (case#2 and case#4) the corresponding α_d^e (eutectic) inside the CET surface decreases from 0.078 to 0.037 in account of solid fraction α_s^e . Accordingly, the concentration of equiaxed dendrite envelope, c_e , decreases 0.039 to 0.0257. Analogous correlation is achieved between case#3 and case#5. Since φ_{sph}^e is almost the same for case#2&3 and for case#4&5, the calculated α_d^e and c_e are very close for each pair.

Table 2. Calculated average of some phase quantities in ingot and inside the CET surface.

	f_e -ingot	f_c -ingot	α_d^e -core	α_s^e -core	c_e -core
Case#1	0.252	0.711	0.012	0.987	0.0170
Case#2	0.35	0.647	0.078	0.919	0.0390
Case#3	0.311	0.663	0.073	0.925	0.0370
Case#4	0.216	0.778	0.037	0.959	0.0257
Case#5	0.236	0.731	0.033	0.966	0.0252

The calculated solute concentration of phase mixture is used to study the influence of φ_{env}^e and φ_{sph}^e on macrosegregation. A comparison between the simulation results using theoretical and experimental morphological parameters (case#2 and case#4, respectively) is shown in 4. Both exhibit macrosegregation. However, the latter case is much severe. Compared to the measured macrosegregation map [14], the predicted macrosegregation using morphological parameters from experiment (case#4) exhibit better agreement. Thus the range and distribution of Cu concentration are quite similar. The higher negative macrosegregation of case#4 inside the CET surface can be simply attributed to the reduced eutectic content within equiaxed grain envelope (α_d^e in table 2) as discussed above. The higher positive segregation in case#4 can also be related to φ_{sph}^e . The solute rejected from the interdendritic liquid enriches the extradendritic liquid which accumulates due to melt convection in specific regions and solidifies as eutectic causing positive macrosegregation.

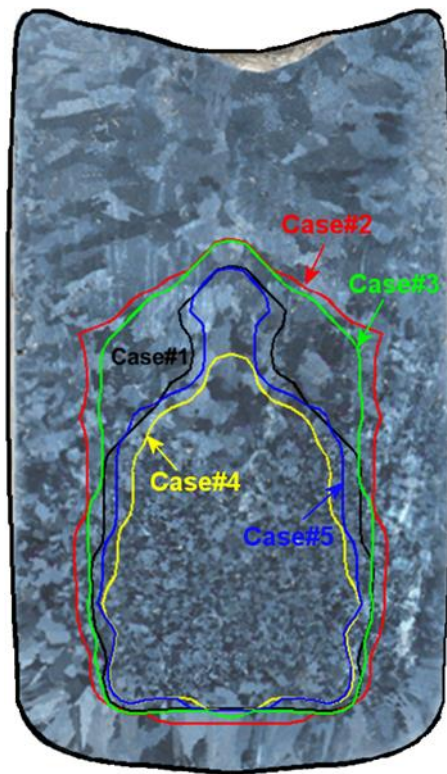


Figure 5. Calculated CET using different morphological parameters as listed in Table 1.

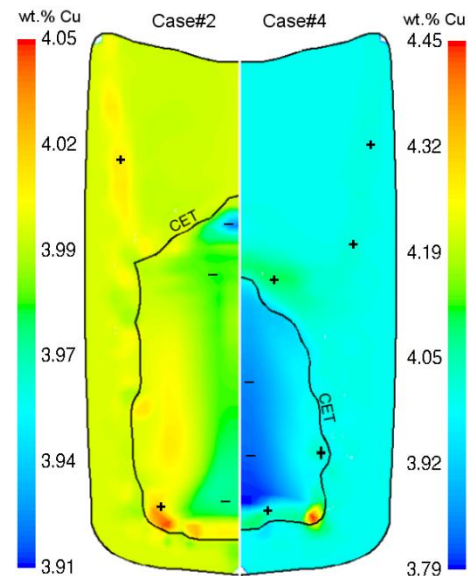


Figure 6. Calculated segregation map with CET for cases #2 and #4.

5. Summary

Shape factor and sphericity of equiaxed dendrite envelope can be extracted from the in situ observation of solidification experiments. In general, φ_{env}^e and φ_{sph}^e vary with time but φ_{sph}^e tends to decrease. The calculated average over time of 4 crystals was $\bar{\varphi}_{env}^e = 0.358$ and $\bar{\varphi}_{sph}^e = 0.623$. The measured φ_{env}^e and φ_{sph}^e are relatively lower than the theoretical values from literature. The comparative numerical study shows that CET configuration and the phase quantities are considerably affected by the morphological parameters. However, the variation is not so dramatic. Decreasing φ_{env}^e reduces envelope growth rate and correspondingly the formed equiaxed phase fraction. Smaller φ_{sph}^e exhibits greater diffusion area and flux through the fictitious grain envelope. Correspondingly, eutectic fraction and solute concentration in equiaxed crystals decrease. Thus the macrosegregation map is also affected by the morphological parameters. The calculated macrosegregation using the experimental morphological parameters fits better to the measurements. Future improvements can be done by using φ_{env}^c and φ_{circ}^c estimated from experiments and to study the influence of cooling conditions on the envelope evolution and shape factors. Numerically, variable morphological parameters have to be implemented in the current model.

Acknowledgement

This work is financially supported by the FWF Austrian Science Fund (P23155-N24).

References

- [1] Beckermann C and Viskanta R 1993 *Applied Mechanics Reviews* **46** 1
- [2] Wang C.Y and Beckermann C 1997 *Metall. Mater. Trans. A* **27** 2754
- [3] Rappaz M and Thévoz P.h 1987 *Acta Metallurgica* **35** 1487
- [4] Rappaz M 1989 *Inter. Mater. Rev.* **34** 93
- [5] Wang C.Y and Beckermann C 1994 *Metall. Mater. Trans. A* **25** 1081
- [6] Martorano M.A, Beckermann C and Gandin Ch-A 2003 *Metall. Mater. Trans. A* **34** 1657

- [7] Ciobanas A.I and Fautrelle Y 2007 *J. Physics D* **40** 3733
- [8] Ludwig A and Wu M 2005 *Metall. Mater. Trans. A* **413** 109
- [9] Wu M and Ludwig A 2006 *Metall. Mater. Trans. A* **37** 1613
- [10] Wu M and Ludwig A 2007 *Metall. Mater. Trans. A* **38** 1465
- [11] Wu M and Fjeld A Ludwig 2010 *Comput. Mater. Sci.* **50** 32
- [12] Wu M and Ludwig A Fjeld A 2010 *Comput. Mater. Sci.* **50** 43
- [13] Wu M, Ahmadein M, Kharicha A, Ludwig A, Li J.H and Schumacher P 2012 *13th MCWASP* (Schladming: Austria) IOP Conf. Ser.: Mater. Sci. Eng. 33
- [14] Ahmadein M, Wu M, Li J.H, Schumacher P and Ludwig A 2013 *Metall. Mater. Trans. A* **44A** 2895
- [15] Ahmadein M, Wu M, Stefan-Kharicha M, Kharicha A and Ludwig A 2014 *Mater. Sci. Forum* **790-791** 247
- [16] Kurz W and Fisher D.J 1998 *Fundamentals of Solidification* 4th ed (Zurich: Trans Tech)
- [17] Lipton J, Glicksman M.E and Kurz W 1984 *Mater. Sci. Eng.* **65** 57
- [18] Thevoz Ph and Rappaz M 1989 *Metall. Trans. A* **20A** 311
- [19] Rappaz M and Gandin Ch.-A 1993 *Acta Metallurgica et Materialia* **41** 345
- [20] Wu M and Ludwig A 2009 *Acta Mater.* **57** 5621
- [21] Hunt J 1984 *Mater. Sci. Eng.* **65** 75
- [22] Bogno A, Nguyen-Thi H, Reinhart G, Billia B and Baruchel J 2013 *Acta Mater.* **61** 1303
- [23] Nguyen-Thi H, Jamgotchian H, Gastaldi J, Härtwig J, Schenk T, Klein H, Billia B, Baruchel J and Dabo Y 2003 *J Phys D: Appl. Phys.* **36** A83
- [24] Buffet A, Nguyen-Thi H, Bogno A, Schenk T, Mangelinck-Noël N, Reinhart G, Bergeon N, Billia B and Baruchel J 2010 *Mater Sci Forum* **649** 331–336